Robustness and Adaptability Analysis for Equivalent Model of Doubly Fed Induction Generator Wind Farm Using Measured Data

Zhang Jian, Cui Mingjian*, He Yigang*

ABSTRACT: As many large wind farms connected to the power grid, it is necessary to develop a robust and adaptable dynamic equivalent model of the wind farm for system analysis and control. In this paper, the trajectory sensitivity of time-varying parameters of the equivalent model is analyzed. Then the non-time-varying parameters of the equivalent model are fixed as aggregated values, while the time-varying parameters are identified using the genetic learning particle swarm optimization based on phasor measurement unit data at the point of interconnection. The robustness and adaptability of the equivalent model under different scenarios are analyzed. The simulation results using the Western Electricity Coordinating Council benchmark test system show that the global searching capability to find the optimal point of the proposed method is higher than canonical particle swarm optimization and genetic algorithm by 2 orders. Further, the biggest mismatch between the identification results of the proposed method and the true values is within 10% for parameters with high sensitivity which is much better than previous work.

KEY WORDS : doubly fed induction generators (DFIG) wind farm; equivalent model of wind farm; trajectory sensitivity; parameters identification; genetic learning particle swarm optimization (GLPSO) hybrid algorithm

1 Introduction

At present, fossil energy shortage, serious environmental pollution, and global climate change have caused worldwide renewable energy revolution, which has led to profound changes in power systems [1].

As typical renewable energy, wind power has the advantages of environmental friendliness, abundance, high energy density and conversion efficiency. It has attracted the attention of all countries. Many countries have accelerated the pace of exploring wind power [2]. Up to date, the installed capacity of wind turbines in China has ranked first in the world.

Large DFIG wind farm has a significant impact on transient stability [3] and small-signal stability [4] of power system. Unlike traditional generators, large wind farm consists of hundreds of wind turbines. It is unrealistic to model each turbine in detail. It is essential to develop a reasonable dynamic equivalent model of a wind farm for power system stability analysis, control algorithm design [5], network planning and relay protection design.

According to the number of equivalent machines, existing methods of representing wind farm can be divided into two categories: single-machine representation method [6,7] and multi-machine representation method [8,9]. According to the data used for modeling, it can be divided into aggregation method based on physical parameters of each wind turbine [10, 11] and parameters identification method based on phasor measurement unit (PMU) data. The idea behind the multi-machine representation method is to cluster wind turbines according to their characteristic parameters such as position, wind speed, slip, stator voltage and real-time power etc. Then wind turbines in the same cluster are aggregated into one equivalent machine. However, different from traditional generators, most of the characteristic parameters of wind turbines are usually unknown. Moreover, the characteristic parameters are dynamically changing, which results in the number and parameters of the developed equivalent model variable. Therefore, it is no longer applicable after a long time. Furthermore, the high computation complexity of clustering makes this method difficult to apply in practice. The single-machine representation method focuses on the dynamic response of the whole wind farm. The complex position distribution, as well as the difference of operation state and electrical interaction between wind turbines, is neglected. Since the whole wind farm is equivalent to one machine, the computing complexity is greatly reduced.

On the other hand, because of the high failure rate of the distribution network, the impedance of wind turbines and distribution networks may deviate greatly from the nominal value after a long time. Moreover, the configurations of distribution network change from time to time, resulting in the change of impedance of the equivalent distribution network. The traditional aggregation method based on detailed physical parameters of each wind turbine and distribution network cannot effectively solve the above parameters -variable problem. Equivalent modeling of the wind farm based on PMU data can make up for this shortcoming, which has attracted the attention of many experts and scholars.

In [12], the reason for the difference between the measured curve of wind farm and the simulation curve of its equivalent model is analyzed. In [13], the dynamic response curves of single-machine and multi-machine representation models are compared and analyzed in terms of descriptive ability. It is pointed out that the single-machine representation model can effectively represent the whole wind farm. In [14], the wide-area trajectory sensitivity for the parameters of the equivalent model of wind farm with constant speed induction generator is computed and analyzed. The genetic algorithm (GA) is used to identify the parameters of the equivalent model aiming at minimizing the total fitting error of wide-area rotor angles of generators. In [15], hybrid dynamic simulation is used to simplify the external system of

the wind farm. Then the PSO gradient search algorithm is used to identify the parameters of the equivalent model of DFIG wind farm. In [16], an improved GA is used to identify the parameters of the equivalent model for the DFIG wind farm. In [17], the DFIG wind turbines are grouped according to their locations. The wind turbines in the same group are aggregated into one equivalent machine. Then oscillation mode analysis is used to verify the validity of the equivalent model. In [18], a linear differential equation is developed for the equivalent model of the DFIG wind farm. Then eigenvalue analysis is used to verify the validity of the equivalent model. In [19], the robustness of the equivalent model for the DFIG wind farm is analyzed. However, the results of parameter identification deviate too much from the true values because the limiting units of control systems for converters are ignored. The identification errors of stator resistance and rotor reactance of an induction generator exceed 50%, and that of rotor resistance exceeds 100%.

None of the above literature has identified the equivalent impedance of the distribution network of the wind farm using PMU data. Since the wind speed of each turbine in the wind farm may be different, the operation state of each wind turbine may be different. Moreover, after long term operation, the impedance of lines and step-up transformers are affected by temperature, geographical environment, vibration, faults, operation configurations and other factors. As a consequence, it may be quite different from the nominal value after a long time. Nevertheless, the equivalent impedance of the distribution network has a great influence on the stability of the power system. Therefore, it needs to be identified accurately. One of the highlights of this paper lies in that the trajectory sensitivity of the equivalent impedance of the distribution network is analyzed and it is added to the parameters to be identified using PMU data.

In this paper, the detailed dynamic equivalent model of DFIG wind farm and initialization method are developed based on PMU data. The trajectory sensitivity of time-varying parameters is analyzed. The time-varying parameters are identified using GLPSO using PMU data. The non-time-varying parameters are fixed as aggregated values. The robustness and adaptability of the developed equivalent model and parameter identification method are validated under different scenarios. These scenarios include different wind speeds, wake effects, off-line conditions of some DFIG, different short circuit locations, depth of voltage sag, and when the wind speed is unknown. The global searching capability to find the optimal point of the proposed algorithm is also compared with the canonical GA and PSO algorithm. The precision of parameters identification results are compared with previous state-of-art work [19].

The originality and contributions of this paper with respect to [19] are as follows: 1) The initialization method of the equivalent model of DFIG wind farm is proposed, in which rotor friction of induction generator is taken into account. 2) How to set the initial values of rotor voltage and slip to overcome convergence problem of power flow calculation is proposed. 3) The trajectory sensitivity of time-varying parameters of the equivalent model is analyzed. It is found that the impedance of the distribution network has the highest sensitivity. 4) The equivalent impedance of the distribution network is identified using PMU data. 5) The role of limiting units in the control system of converters is taken into account in the parameter identification process. 6) The maximum and minimum reference current of limiting units for active and reactive power controllers of machine side converters and voltage controllers of grid side converters are aggregated using the capacity weighted average method. The capacitance of the DC capacitor, the proportional and integral amplification values of the controllers of the equivalent model are also aggregated using this method. 7) The novel GLPSO hybrid algorithm is introduced to identify the key parameters of the equivalent model. Its global searching capability to find optimum point is compared with canonical PSO and GA. 8) The robustness and adaptability of the equivalent model and parameter identification method are addressed for different fault locations, voltage drops and when wind speed is unknown. 9) The precision of parameter identification results are compared with [19]. It is found that the precision of parameter identification results of the proposed method is much higher than [19].

2 Initialization of the equivalent model of DFIG wind farm

The model of DFIG is addressed in many works of literature. In this paper, the DFIG model in [19] is adopted. The steady-state equivalent circuit of DFIG is shown in Fig.1 [20]. Suppose a PMU is installed at the point of interconnection. Still, suppose the steady-state voltage recorded by PMU is $\dot{V}_1$ and active and reactive power injected into power grid are P_1, Q_1 respectively. Assuming the equivalent impedance of the distribution network is $R_t+\mathrm{j}X_t$. The current injected into power grid from the equivalent model is

$$\dot{I}_1 = \frac{P_1 - \mathrm{j}Q_1}{\dot{V}_1^*} \tag{1}$$

where $\dot{V}_1^*$ is the conjugate of $\dot{V}_1$.

The stator voltage of the equivalent DFIG is

$$\dot{V}_s = \dot{V}_1 + \dot{I}_1 \times (R_t + \mathrm{j}X_t) \tag{2}$$

The active and reactive power injected into power grid from the equivalent DFIG are

$$P_0 = P_1 + I_1^2 R_t \tag{3}$$

$$Q_0 = Q_1 + I_1^2 X_t \tag{4}$$

The apparent power on the stator side is

$$S_{\rm sm}=\dot{V}_{\rm s}\dot{I}_{\rm s}^{*}=P_{\rm sm}+{\rm j}Q_{\rm sm}=$$
$$\left(\frac{R_{\rm s}V_{\rm s}^{2}}{R_{\rm s}^{2}+X_{\rm s}^{2}}-V_{\rm s}V_{\rm m}\frac{R_{\rm s}\cos\theta_{\rm sm}-X_{\rm s}\sin\theta_{\rm sm}}{R_{\rm s}^{2}+X_{\rm s}^{2}}\right)+{\rm j}\left(\frac{X_{\rm s}V_{\rm s}^{2}}{R_{\rm s}^{2}+X_{\rm s}^{2}}-V_{\rm s}V_{\rm m}\frac{X_{\rm s}\cos\theta_{\rm sm}+R_{\rm s}\sin\theta_{\rm sm}}{R_{\rm s}^{2}+X_{\rm s}^{2}}\right)\quad(5)$$

$$S_{\rm ms}=-\dot{V}_{\rm m}\dot{I}_{\rm s}^{*}=P_{\rm ms}+{\rm j}Q_{\rm ms}=$$
$$\left(\frac{R_{\rm s}V_{\rm m}^{2}}{R_{\rm s}^{2}+X_{\rm s}^{2}}-V_{\rm m}V_{\rm s}\frac{R_{\rm s}\cos\theta_{\rm ms}-X_{\rm s}\sin\theta_{\rm ms}}{R_{\rm s}^{2}+X_{\rm s}^{2}}\right)+{\rm j}\left(\frac{X_{\rm s}V_{\rm m}^{2}}{R_{\rm s}^{2}+X_{\rm s}^{2}}-V_{\rm m}V_{\rm s}\frac{X_{\rm s}\cos\theta_{\rm ms}+R_{\rm s}\sin\theta_{\rm ms}}{R_{\rm s}^{2}+X_{\rm s}^{2}}\right)\quad(6)$$

The apparent power of the supply side converter is

$$S_{\rm sg}=-\dot{V}_{\rm s}\dot{I}_{\rm g}^{*}=P_{\rm sg}+{\rm j}Q_{\rm sg}=$$
$$\left(\frac{R_{\rm T}V_{\rm s}^{2}}{R_{\rm T}^{2}+X_{\rm T}^{2}}-V_{\rm s}V_{\rm g}\frac{R_{\rm T}\cos\theta_{\rm sg}-X_{\rm T}\sin\theta_{\rm sg}}{R_{\rm T}^{2}+X_{\rm T}^{2}}\right)+{\rm j}\left(\frac{X_{\rm T}V_{\rm s}^{2}}{R_{\rm T}^{2}+X_{\rm T}^{2}}-V_{\rm s}V_{\rm g}\frac{X_{\rm T}\cos\theta_{\rm sg}+R_{\rm s}\sin\theta_{\rm sg}}{R_{\rm T}^{2}+X_{\rm T}^{2}}\right)\quad(7)$$

$$S_{\rm gs}=\dot{V}_{\rm g}\dot{I}_{\rm g}^{*}=P_{\rm gs}+{\rm j}Q_{\rm gs}=$$
$$\left(\frac{R_{\rm T}V_{\rm g}^{2}}{R_{\rm T}^{2}+X_{\rm T}^{2}}-V_{\rm g}V_{\rm s}\frac{R_{\rm T}\cos\theta_{\rm gs}-X_{\rm T}\sin\theta_{\rm gs}}{R_{\rm T}^{2}+X_{\rm T}^{2}}\right)+{\rm j}\left(\frac{X_{\rm T}V_{\rm g}^{2}}{R_{\rm T}^{2}+X_{\rm T}^{2}}-V_{\rm g}V_{\rm s}\frac{X_{\rm T}\cos\theta_{\rm gs}+R_{\rm s}\sin\theta_{\rm gs}}{R_{\rm T}^{2}+X_{\rm T}^{2}}\right)\quad(8)$$

The reactive power absorbed by the excitation winding is

$$S_{\rm mm}={\rm j}Q_{\rm mm}={\rm j}V_{\rm m}^{2}/X_{\rm m}\quad(9)$$

The apparent power of the rotor winding is

$$S_{\rm mr}=-\dot{V}_{\rm m}\dot{I}_{\rm r}^{*}=P_{\rm mr}+jQ_{\rm mr}=$$
$$\left(\frac{sR_{\rm r}V_{\rm m}^{2}}{R_{\rm r}^{2}+s^{2}X_{\rm r}^{2}}-V_{\rm m}V_{\rm r}\frac{R_{\rm r}\cos\theta_{\rm mr}-sX_{\rm r}\sin\theta_{\rm mr}}{R_{\rm r}^{2}+s^{2}X_{\rm r}^{2}}\right)+{\rm j}\left(\frac{s^{2}X_{\rm r}V_{\rm m}^{2}}{R_{\rm r}^{2}+s^{2}X_{\rm r}^{2}}-V_{\rm m}V_{\rm r}\frac{sX_{\rm r}\cos\theta_{\rm mr}+R_{\rm r}\sin\theta_{\rm mr}}{R_{\rm r}^{2}+s^{2}X_{\rm r}^{2}}\right)\quad(10)$$

$$S_{\rm rm}=\dot{V}_{\rm r}\dot{I}_{\rm r}^{*}=P_{\rm rm}+{\rm j}Q_{\rm rm}=$$
$$\left(\frac{R_{\rm r}V_{\rm r}^{2}/s}{R_{\rm r}^{2}+s^{2}X_{\rm r}^{2}}-V_{\rm r}V_{\rm m}\frac{sR_{\rm r}\cos\theta_{\rm rm}-s^{2}X_{\rm r}\sin\theta_{\rm rm}}{R_{\rm r}^{2}+s^{2}X_{\rm r}^{2}}\right)+{\rm j}\left(\frac{sX_{\rm r}V_{\rm r}^{2}}{R_{\rm r}^{2}+s^{2}X_{\rm r}^{2}}-V_{\rm r}V_{\rm m}\frac{s^{2}X_{\rm r}\cos\theta_{\rm rm}+sR_{\rm r}\sin\theta_{\rm rm}}{R_{\rm r}^{2}+s^{2}X_{\rm r}^{2}}\right)\quad(11)$$

On a steady state, the power flow equations of the equivalent DFIG are

$$\Delta P_{\rm s}=P_0-P_{\rm sm}-P_{\rm sg}=0\quad(12)$$
$$\Delta Q_{\rm s}=Q_0-Q_{\rm sm}-Q_{\rm sg}=0\quad(13)$$
$$\Delta P_{\rm m}=-P_{\rm ms}-P_{\rm mr}=0\quad(14)$$
$$\Delta Q_{\rm m}=-Q_{\rm ms}-Q_{\rm mm}-Q_{\rm mr}=0\quad(15)$$
$$\Delta P_{\rm g}=-P_{\rm rm}-P_{\rm gs}=0\quad(16)$$
$$\Delta Q_{\rm g}=Q_{\rm g,set}-Q_{\rm gs}=0\quad(17)$$

$$\Delta P_{\rm wt}=P_0+(P_{\rm sm}^{2}+Q_{\rm sm}^{2})R_{\rm s}/V_{\rm s}^{2}+(P_{\rm mr}^{2}+Q_{\rm mr}^{2})R_{\rm r}/V_{\rm m}^{2}+(P_{\rm gs}^{2}+Q_{\rm gs}^{2})R_{\rm g}/V_{\rm g}^{2}+F(1-s)^{2}-P_{\rm wt}=0\quad(18)$$

$$P_{\rm wt}=k_{\rm opt}(1-s)^{3}\quad(19)$$

where $Q_{\rm g,set}$ is the reference value for reactive power of grid side converter, generally set to be 0. $k_{\rm opt}$ is a constant, determined by the physical parameters of DFIG. F is the friction factor of the rotor.

The Newton-Raphson method can be used to solve (5)~(19). As a result, $V_{\rm m}\angle\theta_{\rm m}$, $V_{\rm r}\angle\theta_{\rm r}$, $V_{\rm g}\angle\theta_{\rm g}$, s can be obtained.

The following currents can be obtained according to the equivalent circuit of Fig. 1.

$$\dot{I}_{\rm r}=(\dot{V}_{\rm r}/s-\dot{V}_{\rm m})/(R_{\rm r}/s+{\rm j}X_{\rm r})\quad(20)$$
$$\dot{I}_{\rm s}=(\dot{V}_{\rm m}-\dot{V}_{\rm s})/(R_{\rm s}+{\rm j}X_{\rm s})\quad(21)$$
$$\dot{I}_{\rm g}=(\dot{V}_{\rm g}-\dot{V}_{\rm s})/(R_{\rm T}+{\rm j}X_{\rm T})\quad(22)$$

It is worth pointing out that the initial values of rotor voltage $V_{\rm r}$ and its phase angle $\theta_{\rm r}$ can be set according to (23), (24) to avoid convergence problem. The slip s usually takes a value in the interval [-0.3 0.4]. If the symbols of s (positive or negative) cannot be determined in advance, it can be assumed to be positive. Then the initial value of it can be set certain positive figures in the interval (0 0.4]. After that, the power flow calculation can be carried out by setting the initial values of $V_{\rm r}$, $\theta_{\rm r}$ according to (23) and (24). Generally, the power flow calculation converges within 10 iterations. If s and $V_{\rm r}$ finally converge to negative values after power flow calculation, this does not mean the voltage magnitude of the rotor is negative. It means that the voltage phase of the rotor of the power flow calculation result should be increased by 180°.

$$\theta_{\rm r}=\theta_{\rm s}\quad(23)$$
$$V_{\rm r}=s\quad(24)$$

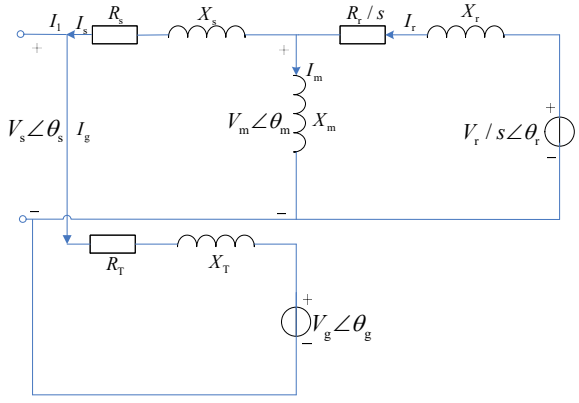

Fig. 1 Steady-state equivalent circuit of DFIG

3 Trajectory sensitivity of time-varying parameters of the equivalent model

There are dozens of parameters in the equivalent model of the DFIG wind farm. Different parameters

have different effects on the dynamic characteristics of the power system. If all parameters are identified, it will take too much computing time. Moreover, the identification results will be very dispersive and difficult to be applicated in practice. Therefore, only the key parameters need to be identified. In [19], it is pointed out that the key parameters consist of resistance and reactance of stator and rotor, and reactance of excitation windings for the induction generator. Further, since the non-time-varying parameters can be fixed as aggregated values, only the time-varying parameters need to be identified. Since the equivalent impedance of the distribution network is time-varying, if its sensitivity is high, it must be identified using PMU data. To address this, the sensitivity analysis of stator and rotor resistance, reactance, excitation reactance of induction generator and distribution network impedance is carried out according to (3) and (4) in [16].

The sensitivity of time-varying parameters of the equivalent model of DFIG wind farm is investigated using the simulation system shown in Fig.2. There are 6 DFIG in the wind farm. The rated active power of each DFIG is 1.5MW. The rated power factor is 0.9. The parameters of each DFIG are shown in Table V and VI in the appendix of [19]. The rated capacity of transformer T2 is 12 MVA and the resistance and leakage reactance of T2 are 0.0018 p.u. and 0.05 p.u. respectively. A three-phase short circuit fault is set at the midpoint of line L1. The fault duration is set to be 0.15 seconds and the simulation duration is set to be 0.5 seconds.

Each time-varying parameter is increased by 5% in turn according to Table V in the appendix of [19]. The trajectories sensitivity of active and reactive power of the time-varying parameters are calculated and shown in Fig.3 and 4, respectively. It can be seen that the phases of trajectory sensitivity for stator and rotor reactance are almost the same. The average sensitivity of active and reactive power is shown in Tab.1. It can be seen that the sum of the average sensitivities of active and reactive power of each reactance is greater than each resistance. Among them, the average sensitivity of reactance for the equivalent distribution network is the highest. Moreover, the average sensitivity of resistance for the equivalent distribution network is much higher than that of stator and rotor. Therefore, it is reasonable and necessary to add the equivalent impedance of the distribution network to the identification parameters using PMU data.

Generally, the impedance of the distribution network is much smaller than the stator impedance of the induction generator. For example, in the simulation system shown as Fig.2, the impedance of the distribution network is 0.0018+j0.05 p.u., while the impedance of stator for the induction generator is 0.00706+j0.171 p.u. Since the distribution network is in series with the DFIG wind farm, it could be guessed that the distribution network impedance will have smaller or almost the same sensitivity as stator impedance. However, it is found that the sensitivity of the former is much higher than the latter in this paper. So it is an interesting finding.

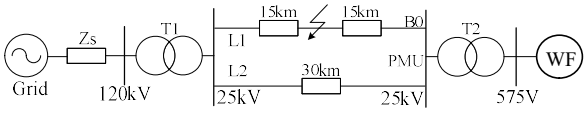

Fig.2 Simulation system

Tab.1 Average trajectory sensitivity of parameters

parameter	P	Q	parameter	P	Q
R_s	0.0348	0.0543	X_r	0.1966	0.4125
R_r	0.0311	0.0071	X_t	0.6765	0.6232
R_t	0.1260	0.1149	X_m	0.0813	0.2388
X_s	0.5755	0.5543			

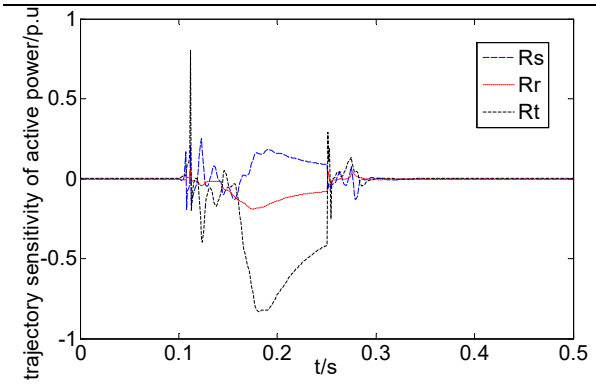

(a) Active power trajectory sensitivity of resistance

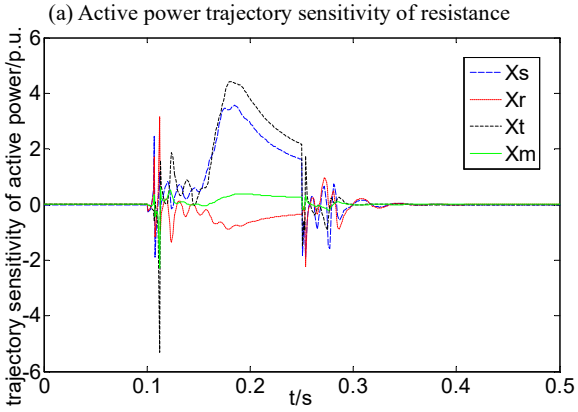

(b) Active power trajectory sensitivity of reactance

Fig.3 Active power trajectory sensitivity

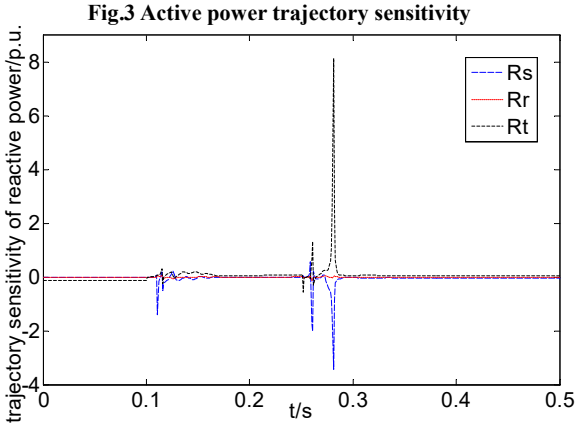

(a) Reactive power trajectory sensitivity of resistance

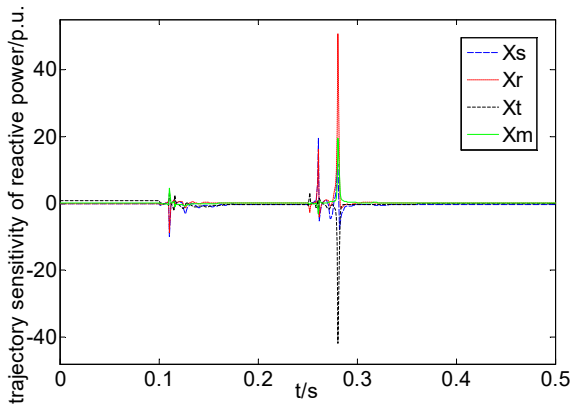

(b) Reactive power trajectory sensitivity of reactance

Fig.4 Reactive power trajectory sensitivity

4 Parameters identification for the equivalent model of DFIG wind farm

4.1 Model of parameters identification

Parameters identification is an optimization process. As shown in (25), the objective function is to minimize the squared difference between the actual output of the wind farm and the equivalent model. Key parameters of the equivalent model are identified by adjusting their estimation values under the constraints of the model frame, state variables and parameters to be identified.

$$\min \int_{t_1}^{t_2} \left[\left| P(\boldsymbol{\theta},\mathbf{X},t) - P_{eq}(\boldsymbol{\theta},\mathbf{X},t) \right|^2 + \left| Q(\boldsymbol{\theta},\mathbf{X},t) - Q_{eq}(\boldsymbol{\theta},\mathbf{X},t) \right|^2 \right] dt \quad (25)$$

$$\text{s.t. } \mathbf{X}_{\min} \le \mathbf{X} \le \mathbf{X}_{\max},\ \boldsymbol{\theta}_{\min} \le \boldsymbol{\theta} \le \boldsymbol{\theta}_{\max}$$

where $P(\boldsymbol{\theta},\mathbf{X},t)$ and $Q(\boldsymbol{\theta},\mathbf{X},t)$ are measured active and reactive power samples of PMU at the points of interconnection under a disturbance. $P_{eq}(\boldsymbol{\theta},\mathbf{X},t)$ and $Q_{eq}(\boldsymbol{\theta},\mathbf{X},t)$ are the active and reactive power output of the equivalent model under the same disturbance. $\mathbf{X}$ is the state variable. $\mathbf{X}_{\min}$ and $\mathbf{X}_{\max}$ are the upper and lower bounds of vector $\mathbf{X}$ respectively. $\boldsymbol{\theta}$ is the vector of key parameters to be identified. $\boldsymbol{\theta}_{\min}$ and $\boldsymbol{\theta}_{\max}$ are the upper and lower bounds of vector $\boldsymbol{\theta}$ respectively, to ensure the rationality of the optimization results.

In [19], the constraints on state variables $\mathbf{X}$ seem to be not taken into account in the model of parameter identification. As a result, the errors of identification results are very large. In this paper, the limit units in the control system of the machine side and the grid side converters are taken into account. The precision of parameter identification results is greatly enhanced.

There are many parameters in the equivalent model. In order to reduce the computational complexity in the process of parameter identification, only the time-varying parameters that have a strong impact on the power system are identified. In this paper, only the resistance and reactance of the stator and rotor, excitation winding reactance of induction generator, and equivalent impedance of distribution network are identified. In the identification process, because the control system parameters and shafting parameters are non-time-varying parameters, they are fixed as aggregated values.

4.2 Parameters identification algorithm

GA and PSO are very popular algorithms [21]. They have been widely used in optimal power flow, reactive power optimization, voltage control, economic dispatch, and other fields. However, the shortcomings of both algorithms are also very obvious. For example, because crossover and mutation of GA are random, the convergence rate is slow. The global search capability to find the optimum point of PSO is weak. It is easy to fall into local optimum result in premature. In order to overcome the above shortcomings of GA and PSO, many experts and scholars have proposed a variety of hybrid algorithms combining GA and PSO.

In general, the parallel framework is adopted in the conventional GA-PSO hybrid algorithm. Unlike that, the cascade framework is utilized in the GLPSO hybrid algorithm [22]. In the GLPSO hybrid algorithm, exemplars generated by crossover, mutation and selection are provided to particle swarm to update velocity and location. Then experiences accumulated by particle swarm during foraging are provided as genetic material for gene operation. This cycle iterates over and over until the end condition is satisfied. Because positive feedback mechanisms can be produced in a cascade frame, the convergence rate and global searching capability are greatly improved. As a result, the effect of "1+1>2" is achieved. Due to the desirable characteristics, the GLPSO hybrid algorithm in [22] is adopted in this paper.

4.3 Aggregation of non-time-varying parameters

In this paper, only non-time-varying parameters are aggregated, including parameters of mechanical shafting and control systems, etc.

1) Equivalent parameters of mechanical shafting

The aggregation method of the total capacity of the equivalent model, the inertia time constant and the rigidity coefficient of the shafting is given by

$$S_{eq} = \sum_{i=1}^{N} S_i \quad (26)$$

$$H_{teq} = \frac{\sum_{i=1}^{N} \left(H_{ti} \times S_i \right)}{S_{eq}} \quad (27)$$

$$H_{geq} = \frac{\sum_{i=1}^{N} \left(H_{gi} \times S_i \right)}{S_{eq}} \quad (28)$$

$$D_{teq} = \frac{\sum_{i=1}^{N} \left(D_{ti} \times S_i \right)}{S_{eq}} \quad (29)$$

where N is the number of online DFIG wind farms. H_t and H_g are the inertia time constants of wind turbines and generators. D_t is the rigidity coefficient of the shafting system. S_i is the capacity of the i^{th} DFIG online. In this paper, H_t and D_t are not separated. H is used to expressing the total inertia time constant, $H = H_t + H_g$.

2) Equivalent parameters of control systems

Shown as (30) and (31), proportional and integral amplification values of the controllers for the equivalent model equal to that of the capacity weighted average sum of each DFIG.

$$K_{Peq}=\frac{\sum_{i=1}^{N}\left(K_{Pi}\times S_i\right)}{S_{eq}} \tag{30}$$

$$K_{Ieq}=\frac{\sum_{i=1}^{N}\left(K_{Ii}\times S_i\right)}{S_{eq}} \tag{31}$$

The maximum and minimum reference current of limiting units for active and reactive power controllers of machine side converters and voltage controllers of grid side converters are aggregated as follows.

$$\overline{I}_{eq}=\frac{\sum_{i=1}^{N}\left(\overline{I}_i\times S_i\right)}{S_{eq}} \tag{32}$$

$$\underline{I}_{eq}=\frac{\sum_{i=1}^{N}\left(\underline{I}_i\times S_i\right)}{S_{eq}} \tag{33}$$

where $\overline{I}$ and $\underline{I}$ are the maximum and minimum current for limiting units respectively.

3) Equivalent capacitance of DC capacitor

The capacitance of the DC capacitor of the equivalent model is equal to the sum of that of each DFIG online. The unit is Faraday.

$$C_{eq}=\sum_{i=1}^{N}C_i \tag{34}$$

4) Equivalent wind speed of the equivalent model

According to the power-wind speed curve of DFIG, the wind power of the equivalent model is equal to the sum of the wind power of each DFIG online. Thus the equivalent wind speed of the equivalent model is given by

$$v_{eq}=\mathrm{f}^{-1}\left(\frac{1}{N}\sum_{i=1}^{N}\mathrm{f}\left(v_i\right)\right) \tag{35}$$

where v_i is the wind speed for the i^{th} DFIG. v_{eq} is the equivalent wind speed of the equivalent model. f is the power-wind speed curve of DFIG.

4.4 Application in reality

In reality, the non-time-varying parameters of the equivalent model of DFIG wind farms are fixed to the aggregated values. Then, data samples under disturbance including voltage amplitude, phase angle, active and reactive power recorded by PMU at the point of interconnection are transferred to the equivalent model. Finally, R_s, X_s, R_r, X_r, X_m, R_t, X_t of the equivalent model can be obtained according to Section 2, 4.1, and 4.2.

5 Simulation cases

5.1 Case1

5.1.1 Simulation conditions

The simulation system and its parameters are the same as those in section 3. Set the population size to be 50 and maximum iteration to be 60. Set the coefficients of GLPSO hybrid algorithm as ω=0.7298, sg=7, $pm=0.01$, c=1.49618. The system reference capacity is chosen to be $S_B=S_{eq}=1.5\times 6/0.9$ MVA. The wind speed is set to be 9m/s and the parameter identification interval is set as Tab.2. The program of parameter identification is written in C language. The classic fourth-order Runge-Kutta method is used to solve the differential algebra equations of the dynamic equivalent model of the DFIG wind farm. To avoid the problem of numerical instability, the integration step size is chosen to be 0.00008 seconds. The CPU of the computer is Intel (R) Core (TM) i3-4150 3.5 GHz with 32G RAM.

5.1.2 Simulation results

The parameter identification results are shown in line 2 of Table 3. It can be seen that the identification results are in good agreement with the true values. Only the error of rotor resistance is greater than 10%. This is because the sensitivity of the rotor resistance is lower than other parameters.

To further illustrate the importance of identifying the equivalent impedance of the distribution network, suppose the resistance and leakage reactance of step-up transformer increase by 10% compared with the nameplate data. That is, we suppose after long term operation, the resistance and leakage reactance of step-up transformer is 1.1 times of the nameplate data. In reality, this can happen. Then the equivalent impedance of the distribution network is fixed to the nominal value. Only the stator and rotor resistance, reactance and excitation winding reactance of induction generator are identified. The identification results are shown in line 3 of Tab.3. It can be seen that, due to the difference between the fixed and the true value of the equivalent impedance of the distribution network, the identification error of other parameters increases sharply. The identification error of stator resistance reaches 40% while the identification error of rotor resistance reaches 200%.

Tab.2 Identification intervals of parameters

R_s	X_s	R_r	X_r	X_m	R_t	X_t
[0.0010, 0.0380]	[0.0171, 0.8550]	[0.0010, 0.0250]	[0.0156, 0.7800]	[0.2900, 10.0000]	[0.0008, 0.0030]	[0.0213, 0.0852]

Tab.3 Identification results of parameters

R_s	X_s	R_r	X_r	X_m	R_t	X_t
0.0071	0.1726	0.0043	0.1535	2.96	0.0015	0.0416
0.0049	0.1485	0.0151	0.1872	3.1764	fixed	fixed

5.2 Case2

5.2.1 Simulation conditions

To verify the robustness and adaptability of the proposed equivalent model, the detailed model of the Western Electricity Coordinating Council benchmark test system as shown in Fig. 5 in [19] is developed based on MATLAB. The wind farm consists of 20 DFIG. Each DFIG is connected to a 35kV medium voltage distribution network through a step-up transformer with a rated capacity of 2 MVA. The parameters of each DFIG and the impedance parameters of the step-up transformer are the same as those in [19]. The system reference capacity is chosen to be $S_B=S_{eq}=30/0.9$ MVA when all DFIG are

online. 230 kV transmission network is represented by an infinite voltage source. A three-phase short-circuit with transition resistance 5-ohm fault lasting for 0.15 seconds is set at the middle point of the first line L1. The voltage sag at PMU is about 35%. The simulation time is set to be 0.3 seconds. Other simulation conditions are set the same as 5.1.1.

5.2.2 Simulation results

5.2.2.1Global searching capability and computing efficiency of GLPSO compared with GA and PSO

Set wind speed to be 11 m/s. The program of parameter identification terminates in 116 seconds when the GLPSO hybrid algorithm is adopted. While the program terminated in 104 seconds when canonical GA is adopted and 97 seconds when canonical PSO is adopted. That is, the GLPSO hybrid algorithm is a little slower than canonical GA and PSO.

The base-2 logarithmic values of the objective function for the best individual at each iteration using GLPSO, GA and PSO are shown in Fig.5. It can be seen that the global searching capability to find the optimum point of GLPSO is much stronger than GA and PSO. This is because in GLPSO gene operation is used to increase the diversity and quality of exemplars. As an outcome, genes and experience learning promote each other. Further, as the cascade framework is introduced in GLPSO, the positive feedback mechanism is brought about.

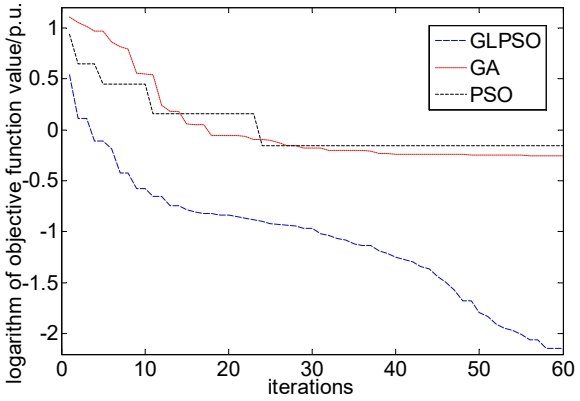

Fig.5 Comparisons of 3 algorithms

5.2.2.2 Robustness and adaptability analysis

1) Dispersion analysis of parameters identification results

The parameter identification results of the equivalent model under the wake effect and various wind speed scenarios are shown in Tab.4. The wind speed settings of each turbine under the wake effect scenario are shown in Tab.5. It can be seen that the dispersion of rotor resistance is larger than other parameters. However, generally speaking, the dispersion of parameter identification results is low.

In reality, some wind turbines may be offline due to overhaul or because the wind speed is lower than the cut-in value. Assume that the turbines 5, 9, 13 and 17 shown as Fig.5 in [19] are offline. Under this circumstance, the system reference capacity is chosen to be $S_B = S_{eq} = 30 \times 0.8/0.9\,\text{MVA}$. The results of parameter identification are shown in Tab. 6. It can be seen that the dispersion of rotor resistance R_r is still somewhat large. The reactance of the stator and rotor also shows some dispersion. But the dispersion of their sum is small. This is because their phase of trajectory sensitivity has some correlation. Other parameters are less dispersive. Generally speaking, the dispersion of results of parameter identification is satisfactory.

Tab.4 Parameter identification results 100% on-line

wind	R_s	X_s	R_r	X_r	X_m	R_t	X_t
7m/s	0.0075	0.1769	0.0071	0.1466	2.8336	0.0018	0.0425
8m/s	0.0071	0.1760	0.0046	0.1473	2.7727	0.0019	0.0424
9m/s	0.0070	0.1782	0.0052	0.1464	2.7519	0.0018	0.0425
10m/s	0.0071	0.1681	0.0063	0.1607	3.0438	0.0021	0.0423
11m/s	0.0070	0.1674	0.0035	0.1586	2.8229	0.0021	0.0434
12m/s	0.0065	0.1622	0.0053	0.1653	2.9336	0.0026	0.0436
wake effect	0.0065	0.1656	0.0086	0.1652	3.10	0.0017	0.0438

Tab.5 Wind speed of DFIG considering wake effect

DFIG	wind	DFIG	wind	DFIG	wind	DFIG	wind
1	14m/s	6	12m/s	11	10m/s	16	9m/s
2	13m/s	7	11m/s	12	9.5m/s	17	8.5m/s
3	12m/s	8	10m/s	13	9m/s	18	8m/s
4	11m/s	9	9m/s	14	8.5m/s	19	7.5m/s
5	10m/s	10	8m/s	15	8m/s	20	7m/s

Tab.6 Parameter identification results 80% online

wind	R_s	X_s	R_r	X_r	X_m	R_t	X_t
7m/s	0.0075	0.1778	0.0077	0.1465	2.7813	0.0017	0.0419
9m/s	0.0067	0.1437	0.0080	0.1836	2.9627	0.0018	0.0425
12m/s	0.0070	0.1688	0.0019	0.1555	3.0718	0.0026	0.0437
wake effect	0.0071	0.1892	0.0057	0.1354	2.8234	0.0019	0.0429

2) Verification of descriptive capability of the equivalent model

The fitting curves of active and reactive power when wind speed is 8m/s, 9m/s, 10m/s, and 11m/s are shown in Fig. 6. It can be seen that the fitting effect is good. Therefore, the descriptive capability of the equivalent model is good.

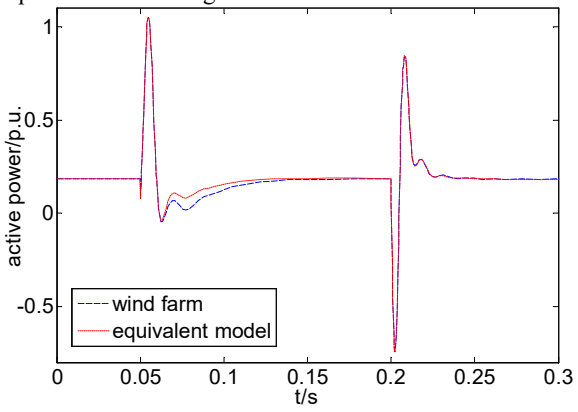

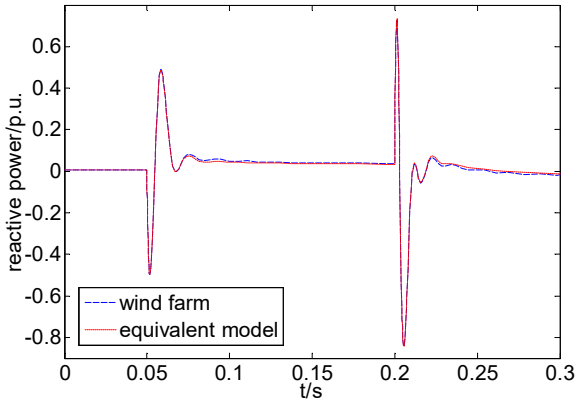

(a) Responses comparison when wind speed is 8m/s

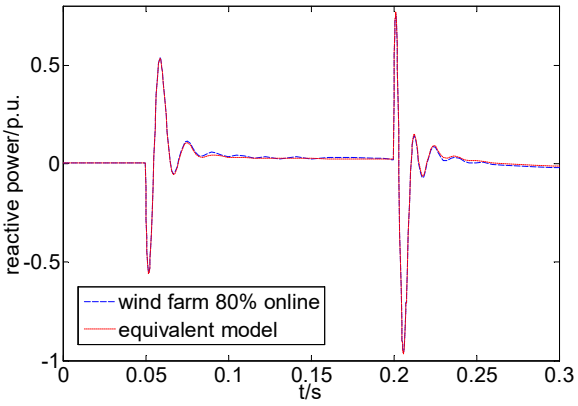

(b) Responses comparison when wind speed is 9m/s

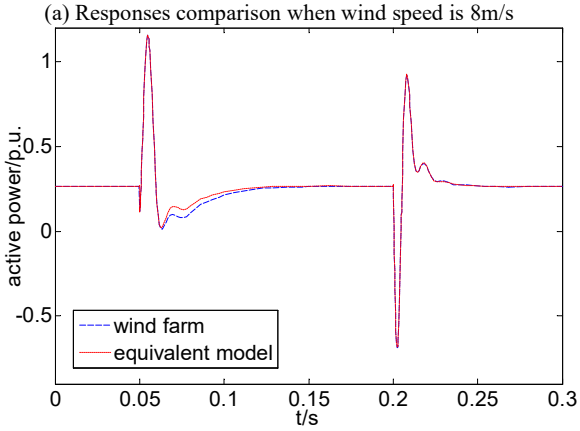

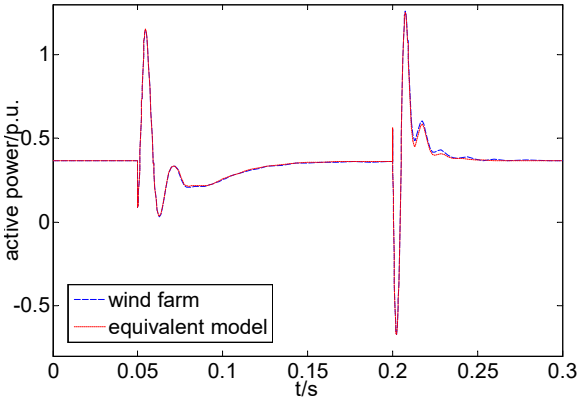

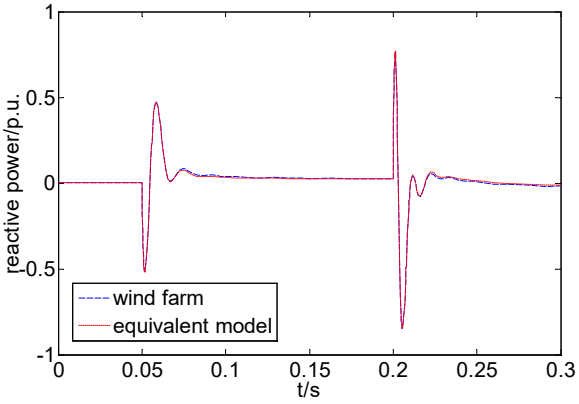

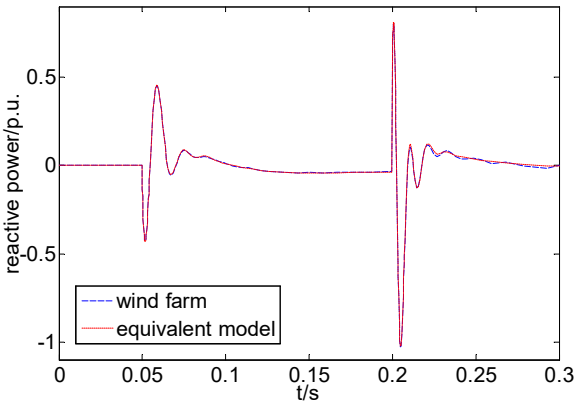

(c) Responses comparison when wind speed is 10m/s

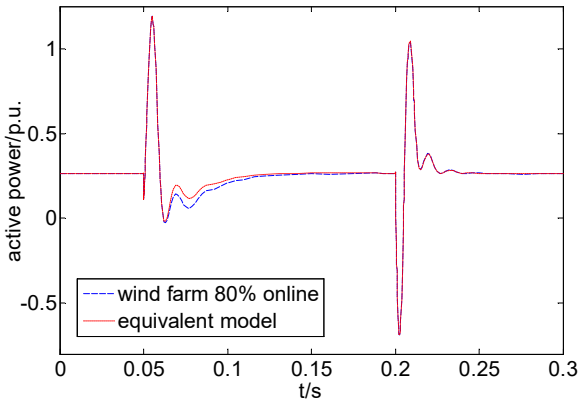

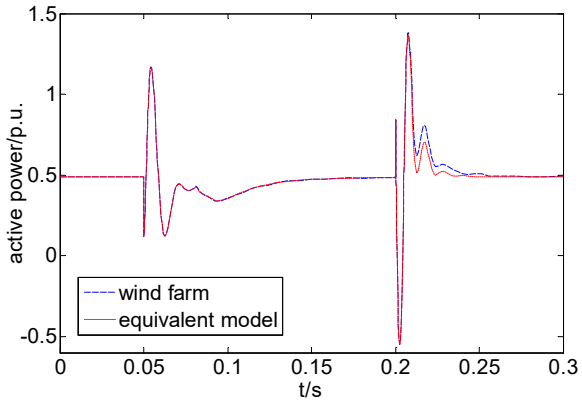

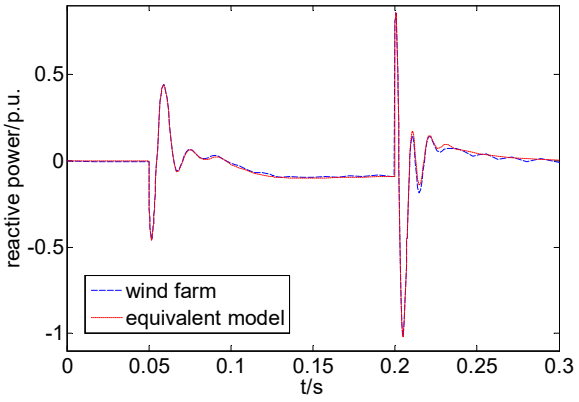

(d) Responses comparison when wind speed is 11m/s

Fig.6 Descriptive capability of the equivalent model

3) Verification of generalization capability for equivalent model

In this paper, the conception of goodness of fit shown as (10) in [19] is used to evaluate the fitting degree between the simulation results of a detailed model of the wind farm and the developed dynamic equivalent model.

Parameters of the equivalent model identified using data samples when wind speed is 9m/s is used to fit the data samples when wind speed is 7m/s, 12m/s, wake effect is considered and 20% wind turbines are offline. The fitting curves are shown in Fig.7. It can be seen that the fitting effect is good. Under the above scenarios, the goodness of fit for active and reactive power is shown in Tab.7. It can be seen that the coincidence is good. Therefore, the generalization capability of the equivalent model is good.

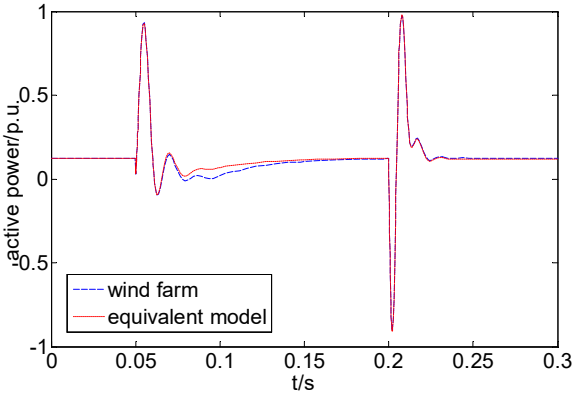

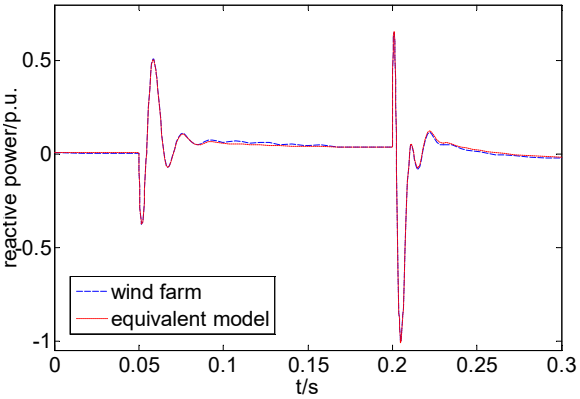

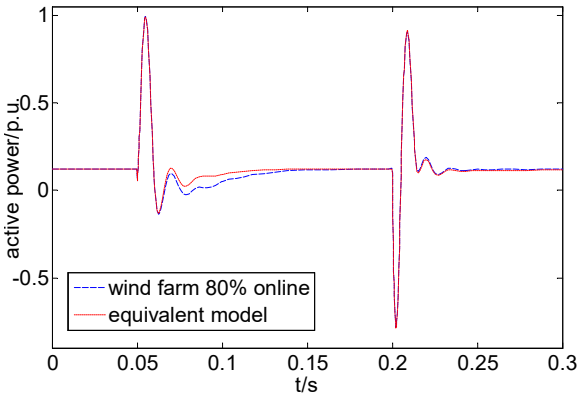

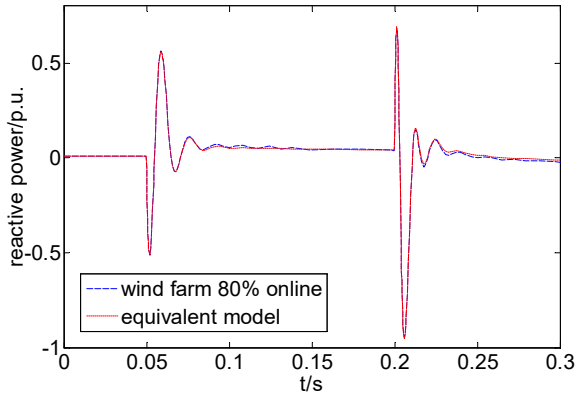

(a) Responses comparison when wind speed is 7m/s

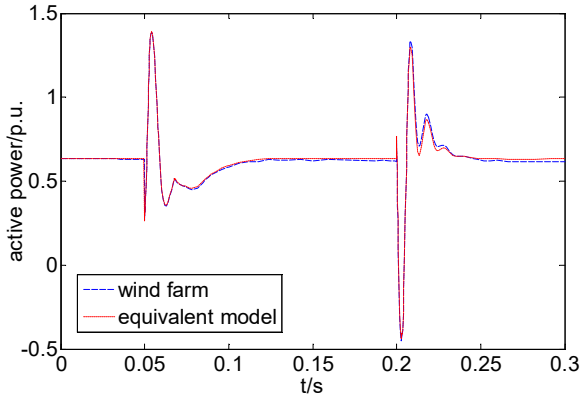

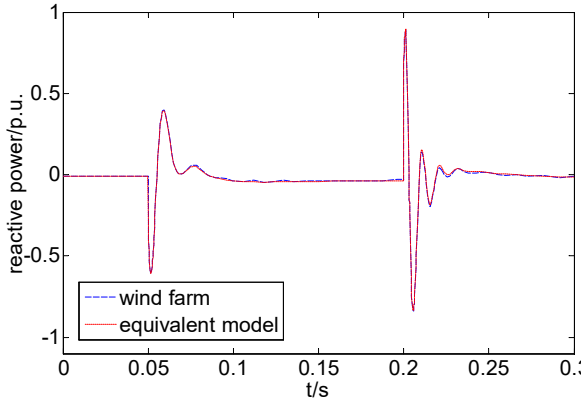

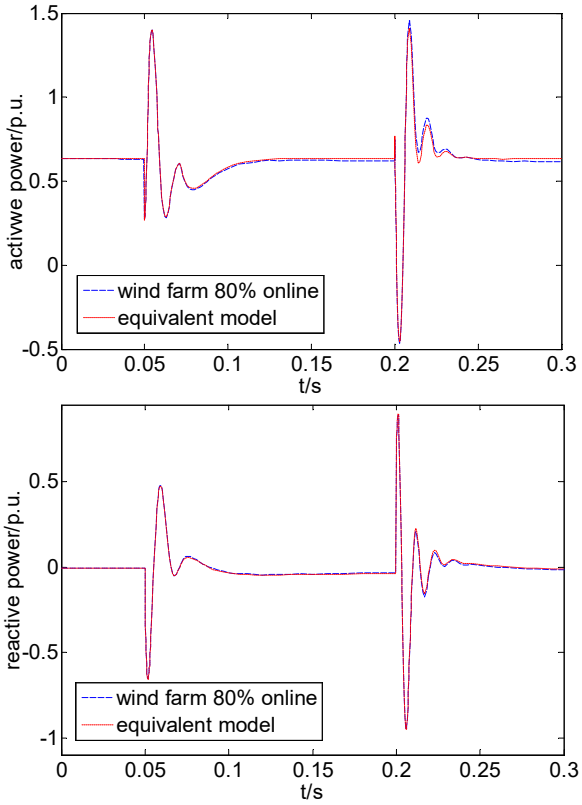

(b) Responses comparison when wind speed is 12m/s

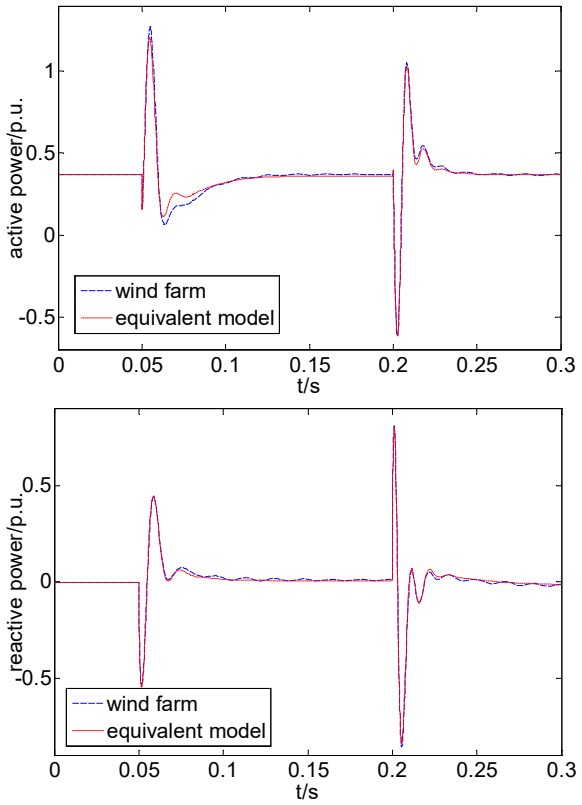

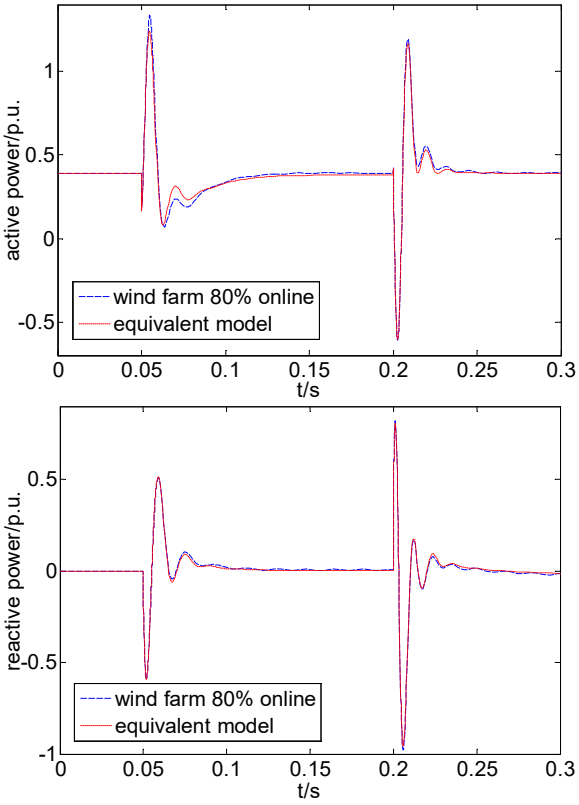

(c) Responses comparison considering wake effect

Fig.7 Generalization capability of the equivalent model

Tab.7 Comparisons of fitting curves of equivalent model

100% online	P	Q	80% online	P	Q
7m/s	97.5221%	98.9433%	7m/s	97.8625%	98.4320%
12m/s	98.4911%	98.7342%	12m/s	98.5112%	98.7625%
Wake effect	97.6241%	98.7542%	Wake effect	97.4123%	98.6925%

4) Unknown wind speed scene

Assuming that there is not any wind measuring equipment installed in the wind farm. The mechanical input torque of each turbine can be approximately considered to be constant in the transient process. Therefore, it can be assumed that the input mechanical torque of the equivalent model is constant and fixed as the steady-state value of power flow calculation. The results of parameter identification using this method are shown in Tab.8. It can be seen that the results for identified resistances are more dispersive than those in Tab.4. However, the identification results of equivalent distribution network reactance, excitation wingding reactance and the sum of stator and rotor reactance are still stable and satisfactory.

Tab.8 Identification results if wind speed is unknown

Wind	R_s	X_s	R_r	X_r	X_m	R_t	X_t
7m/s	0.0084	0.1733	0.0051	0.1512	2.8732	0.0010	0.0426
8m/s	0.0072	0.1777	0.0057	0.1425	2.7946	0.0018	0.0423
9m/s	0.0079	0.1923	0.0048	0.1347	2.7248	0.0011	0.0425
10m/s	0.0079	0.1701	0.0035	0.1546	2.8455	0.0010	0.0436
11m/s	0.0080	0.1667	0.0106	0.1565	3.0012	0.0012	0.0441
12m/s	0.0054	0.1471	0.0010	0.1846	3.0543	0.0029	0.0451
Wake effect	0.0090	0.1729	0.0236	0.1515	3.3031	0.0016	0.0460

5) Parameter identification results for different fault locations and voltage sag depths

The wind speed of each DFIG is set to be 9 m/s. A three-phase short-circuit through 10 and 8-ohm transition resistors at the middle point of line L1 are set respectively. The corresponding voltage sags depths at PMU are about 12% and 19% respectively. The results of parameter identification are shown in rows 2 and 3 of Tab.9 respectively. Another three-phase short-circuit through 5-ohm transition resistance at the sending end of line L1 is set. The corresponding voltage sag at PMU is about 25%. The results of parameter identification are shown in rows 4 of Tab.9. It can be seen that the results of parameter identification are very close under three different fault locations or voltage sag depths.

Tab.9 Identification results under different fault locations and depth of voltage sags

voltage sags	R_s	X_s	R_r	X_r	X_m	R_t	X_t
12%	0.0074	0.1724	0.0077	0.1565	2.8422	0.0014	0.0427
19%	0.0073	0.1705	0.0064	0.1551	2.8137	0.0014	0.0428
25%	0.0072	0.1736	0.0059	0.1567	2.9224	0.0015	0.0427

6) Comparisons with previous state-of-art work

For the sake of comparison fairness, the equivalent impedance of the distribution network is fixed to the value as Table I in [19]. Set wind speed to be 9m/s and maximum iterations of GLPSO to be 30. Other simulation conditions are set the same as 5.2.1. The identification results compared with [19] are shown as Tab.10. It can be seen that the identification results of the proposed method in this paper are much closer to the true values than [19]. In addition, the precision of parameters identification results for R_s, R_r, X_r, X_m in Tab.4, Tab.6, Tab.8, Tab.9, are all higher than [19]. The precision of parameter identification results for X_s are close to [19]. On average, the precision of parameter identification results of the proposed method in this paper is much higher than [19].

Tab.10 Identification results compared with previous work

parameters	R_s	X_s	R_r	X_r	X_m
True values	0.00706	0.1710	0.0050	0.1560	2.9000
Reference [19]	0.01150	0.1680	0.0104	0.0804	2.6564
Proposed method	0.00584	0.1684	0.0037	0.1563	3.0187

6 Conclusions

After long term operation, the equivalent dynamic characteristics of a wind farm may be changed due to the changes of distribution network impedance and induction generator parameters. Traditional aggregation methods based on detailed physical parameters of wind farms are not applicable.

Based on phasor measurement unit data at the point of interconnection, the detailed dynamic equivalent model of doubly fed induction generators is developed in this paper. Further, the initialization method to avoid the convergence problem of power flow calculation is proposed. The trajectory sensitivity of time-variable parameters for the equivalent model is analyzed. It is found that the equivalent impedance of the distribution network has very high sensitivity.

The time-varying parameters are identified using a genetic learning particle swarm optimization hybrid algorithm while the non-time-varying parameters are fixed as aggregated values. As a result, the convergence speed and global searching capability to find the optimum point of the program are improved. Moreover, the dispersion of parameter identification results is reduced.

In addition, the robustness and adaptability of the equivalent model are analyzed under different scenarios. The strategy of parameter identification when wind speed is unknown is put forward. Simulation cases indicate that the global searching capability to find the optimal point of the proposed genetic learning particle swarm optimization hybrid algorithm is much higher than canonical particle swarm optimization and genetic algorithm. Furthermore, the precision of parameter identification results is much higher than previous state-of-art work.

In conclusion, the proposed equivalent model and parameters identification method need very little internal information about the wind farm and have excellent adaptability and robustness.

References

[1]Jian Zhang, Mingjian Cui, Hualiang Fang, and Yigang He. Two novel load balancing platforms using common DC buses[J]. IEEE Transactions on Sustainable Energy, 2018, 9(3):1099-1107.

[2]M. Cui, J. Zhang, Estimating ramping requirements with solar friendly flexible ramping product in multi- timescale power system operations, Applied Energy 225 (2018) 27-41.

[3]Jia-Yang Ruan, Zong-Xiang Lu, Ying Qiao, Yong Min, Guang-Hui Shao, Xing-Wei Xu, Kai-Yuan Hou. Transient stability of wind turbine adopting a generic model of DFIG and singularity-induced instability of generators/units with power-electronic interface[J]. IEEE Transactions on Energy Conversion, 2015, 30 (3): 1069-1080.

[4]Durga Gautam, Vijay Vijttal, Terry Harbour. Impact of increased penetration of DFIG-based wind turbine generators on transient and small signal stability of power systems[J]. IEEE Transactions on Power Systems, 2009, 24(3):1426-1433.

[5]B. Yang, T. Yu, H. Shu, J. Dong, L. Jiang, Robust sliding-mode control of wind energy conversion systems for optimal power extraction via nonlinear perturbation observers, Applied Energy 210 (2018) 711-723.

[6]Vahid Jalili-Marandi, Lok-Fu Pak, Venkata Dinavahi. Real-time simulation of grid-connected wind farms using physical aggregation[J]. IEEE Transactions on Industrial Electronics, 2010, 57(9):3010-3021.

[7]Luis M. Fernandeza, Francisco Juradob, Jose Ramon Saenz. Aggregated dynamic model for wind farms with doubly fed induction generator wind turbines[J].

Renewable Energy, 33(2008), 129-140.

[8]Weixing Li, Pupu Chao, Xiaodong Liang, Jin Ma, Dianguo Xu. A practical equivalent method for DFIG wind farms. IEEE Transactions on Sustainable Energy, 2018, 9 (2):610-620.

[9]Muhammad Ali, Irinel-Sorin Ilie, Jovica V. Milanovic, Gianfranco Chicco. Wind Farm model aggregation using probabilistic clustering[J]. IEEE Transactions on Power Systems, 2013, 28(1):309-316.

[10]Jianxiao Zou, Chao Peng, Hongbing Xu, Yan Yan. A fuzzy clustering algorithm-based dynamic equivalent modeling method for wind farm with DFIG. IEEE Transactions on Energy Conversion, 2015, 530(4):1329-1337.

[11]Peng Wang, Zhenyuan Zhang, Qi Huang, Ni Wang, Xing Zhang, Wei-Jen Lee. Improved wind farm aggregated modeling method for large-scale power system stability studies. IEEE Transactions on Power Systems, 2018, 33(6):6332-6342.

[12]Yingchen Zhang, Eduard Muljadi, Dmitry Kosterev, Mohit Singh. Wind power plant model validation using synchrophasor measurements at the point of interconnection. IEEE Transactions on Sustainable Energy, 2015, 6(3):984-991.

[13]J. Brochu, C. Larose, R. Gagnon. Validation of single- and multiple-machine equivalents for modeling wind power plants. IEEE Transactions on Energy Conversion, 2011, 26(2): 532–541.

[14]Jin Lin, Lin Cheng. Model parameters identification method for wind farms based on wide-area trajectory sensitivities. International Journal of Emerging Electric Power Systems. 2010, 11(5), Article 2.

[15]Xueyang Cheng, Weijen Lee, Mandhir Sahni, Yunzhi Cheng, Lyndon K. Lee. Dynamic equivalent model development to improve the operation efficiency of wind farm. IEEE Transactions on Industry Applications, 2016, 52 (4): 2759- 2767.

[16]Yinfeng Wang, Chao Lu, Lipeng Zhu, Guoli Zhang, Xiu Li, Ying Chen. Comprehensive modeling and parameter identification of wind farms based on wide-area measurement systems. Journal of Modern Power Systems and Clean Energy, 2016, 4(3):383–393.

[17]L. P. Kunjumuhammed, B. C. Pal, C. Oates, K. J. Dyke. The adequacy of the present practice in dynamic aggregated modeling of wind farm systems. IEEE Transactions on Sustainable Energy, 2017, 8(1):23-32.

[18]Dong-Eok Kim, Mohamed A El-Sharkawi. Dynamic equivalent model of wind power plant using parameter identification. IEEE Transactions on Energy Conversion, 2016, 31(1):37-45.

[19]Yuhao Zhou, Long Zhao, Wei-Jen Lee. Robustness analysis of dynamic equivalent model of DFIG wind farm for stability Study. IEEE Transactions on Industry Applications, 2018, 54(6):5682-5690.

[20]Shenghu Li. Power flow modeling to doubly-fed induction generators (DFIG) under power regulation[J]. IEEE Transactions on Power Systems, 2013, 28(3):3292-3301.

[21]N. Delgarm, B. Sajadi, F. Kowsary, S. Delgarm, Multi-objective op timization of the building energy performance: A simulation-based approach by means of particle swarm optimization (PSO), Applied Energy 170 (2016) 293–303.

[22]Yuejiao Gong, Jingjing Li, Yicong Zhou, Yun Li, Henry Shuhuang Chung, Yuhui Shi, Jun Zhang. Genetic learning particle swarm optimization. IEEE Transactions on Cybernetics, 2016, 46(10): 2277-2289.